Cation Mobility and the Sorption of Chloroform in Zeolite NaY: Molecular Dynamics Study

Naseem A. Ramsahye and Robert G. Bell*

Davy Faraday Research Laboratory, Royal Institution of Great Britain, 21 Albemarle Street, London, W1S 4BS, United Kingdom

Received: July 9, 2004; In Final Form: December 1, 2004

Molecular dynamics simulations at temperatures of 270, 330, and 390 K have been carried out to address the question of cation migration upon chloroform sorption in sodium zeolite Y. The results show that sodium cations located in different sites exhibit different types of mobility. These may be summarized as follows: (1) SII cations migrate toward the center of the supercage upon sorption, due to interactions with the polar sorbate molecules. (2) SI′ cations hop from the sodalite cage into the supercage to fill vacant SII sites. (3) SI′ cations migrate to other SI′ sites within the same sodalite cage. (4) SI cations hop out of the double six-rings into SI′ sites. In some instances, concerted motion of cations is observed. Furthermore, former SI′ and SI cations, having crossed to SII sites, may then further migrate within the supercage, as in (1). The cation motion is dependent on the level of sorbate loading, with 10 molecules per unit cell not being enough to induce significant cation displacements, whereas the sorption of 40 molecules per unit cell results in a number of cations being displaced from their original positions. Further rearrangement of the cation positions is observed upon evacuation of the simulation cell, with some cations reverting back to sites normally occupied in bare NaY.

Introduction

In recent years, there has been increased interest in aluminosilicate zeolites containing extraframework alkali cations, engendered by their potential applications in base catalysis,[1,2] as well as in the separation and storage of halocarbon molecules, including HFCs.[3−5] Both of these areas of research have been driven by environmental concerns, in the case of halocarbon sorption by the need to obtain purified HFC gases that may act as replacements for ozone-harming CFC coolant gases. In base catalysis, such zeolites are potential alternatives to toxic or corrosive catalysts used in important processes such as the side chain alkylation of toluene to form styrene.[6,7]

In the basic zeolites, aluminum is substituted for silicon in the framework. Alkali metal cations, such as sodium or lithium, compensate the net negative charge left by the substitution of silicon by aluminum and are located in distinct sites in the zeolite pore system. The cations are bound at these sites mainly by electrostatic forces, although they are often conveniently described as being coordinated to one or (usually) more oxygen atoms. The common locations of the cations in dry faujasite-structured zeolites (such as X or Y) are shown in Figure 1, together with the now standard nomenclature for the different sites (SI, SI′ etc.). The basicity of the framework oxygens increases with the number of cations present and with the electropositivity of the cation, with CsX being among the most basic. It is now established, however, that the distribution of the extraframework cations may be substantially perturbed upon adsorption of certain molecules, leading to changes in the framework electron density and in the mode of physical binding of the guest species. This has implications for the sorptive and catalytic properties of the zeolite. In the case of adsorption, increased availability of specific adsorption sites (i.e., cations) could lead to enhanced adsorption of polar or polarizable molecules, resulting also in possible changes in the thermodynamic selectivity. In basic zeolites, the Lewis base sites are attributable to the negatively charged framework oxygen atoms, with the magnitude of the charge being an indicator of the basic strength of that particular site. The charges are partly governed by the Si−O−Al and Si−O−Si angles and the bond lengths between the atoms[2] (i.e., the framework geometry). This in turn will be influenced by the number and siting of the extraframework cations and their possible redistribution during adsorption and catalytic processes. For instance, movement of cations has been deemed to be a key aspect of the activation process for the trimerization of acetylene when using a zeolite catalyst.[8,9] The question of cation mobility is thus crucial in terms of understanding the fundamental chemistry of these materials, and one which has not yet fully been explored, particularly with respect to the precise mechanisms by which the cations migrate.

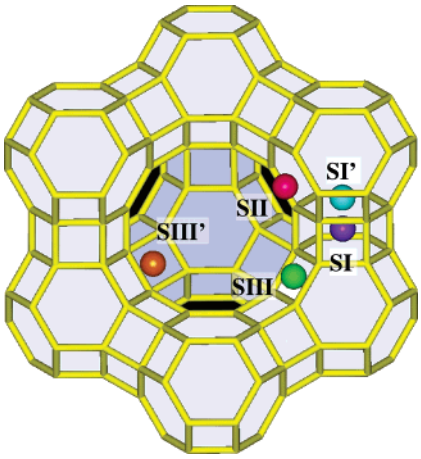

Figure 1. Cation sites and their nomenclature in FAU type zeolites.

* To whom correspondence should be addressed. E-mail rob@ri.ac.uk.

10.1021/jp046958o CCC: $30.25
Published on Web 02/22/2005

Computational techniques provide an invaluable complement to experiments in this regard as they enable explicit modeling of interactions at the atomic level.

Many previous studies, both experimental and computational, have focused on the adsorption of halocarbons in faujasite-structured zeolites. Vibrational spectroscopy and molecular simulations carried out by Mellot, Davidson, and others[10,11] have shed light on the mode of bonding of $CHCl_3$ and other chlorofluorocarbons (CFCs) and hydrofluorocarbons (HFCs) in siliceous FAU, NaY, and NaX. In the X and Y zeolites, the $Na^+\cdots Cl$ (or F) electrostatic interactions dominate, although for H-containing sorbates, H···O(zeolite) hydrogen bonds are also important, in addition to the general sorbate−zeolite van der Waals' interations. Furthermore, X-ray diffraction studies by Grey et al.[12] indicated that migration of Na cations occurred in the case of adsorption of HFC-134 (CHF_2CHF_2) in NaY, finding that SI′ sites in the sodalite cage, normally occupied in the unloaded zeolite, had been vacated, with a corresponding increase in the numbers of cations in the supercage, particularly around the SIII′ sites, and at locations displaced from the SII sites toward the center of the supercage. A more recent structural and computational study[13] found very similar behavior with the sorbate $CFCl_3$.

Chloroform, the subject of our own study, has also been used as a probe sorbate to study the effect of absorption on the cations. Its dipole moment (1.01 D) is such that it can be used to probe cation−anion interactions and also hydrogen−oxygen interactions. Kawai et al.[14] have measured adsorption isotherms of chloroform on NaY at various Si/Al ratios, and from their results, proposed that the main interaction governing chloroform adsorption is a dispersive interaction, although no information on the configurations adopted by the molecules inside the zeolite was given. However, as already touched upon, Monte Carlo simulations by Mellot et al.[11,15,16] showed that both hydrogen−oxygen interactions and chlorine−cation interactions play a role in the adsorption process. The authors also proposed that the preferred binding sites are at the 12 ring windows rather than specifically at SII cation sites.

MAS NMR work on basic zeolites by Bosch et al.[17] and Sanchez-Sanchez et al.[18] indicated possible motion of the sodium cations upon chloroform adsorption. Sanchez-Sanchez et al.[18] concluded that the framework basicity plays a part in the chloroform adsorption. The low field shift of H resonance with increasing framework basicity observed by the authors indicates a hydrogen-bonding interaction, as the nucleophilic framework oxygen polarizes the chloroform molecule. These authors also performed ^{23}Na MAS NMR experiments and calculated the quadrupole coupling constants for the atoms in sites I′ and II. The decrease in these constants upon chloroform sorption was attributed to the migration of sodium cations from site I′ to the site II. Bosch et al.[17] suggested that upon chloroform adsorption, there is a modification of the electron density of the entire zeolite lattice. They concluded from their NMR data that there is a decrease in site I population and an interaction of the chloroform with site II cations. The authors also report that there is an influence on the cations at site SI′, although direct sorbate−cation interaction was ruled out in this case due to the inability of the chloroform molecules to enter the sodalite cage. Hence, the suggestion is that instead the electron distribution on the zeolite lattice is modified.

In this paper, we report molecular dynamics simulations of the adsorption of chloroform on zeolite NaY, carried out to elucidate aspects of the cation migration process. A preliminary report of this study was communicated in a proceeding paper.[19] At around the same time, a very interesting article by Jaramillo et al.[20] appeared, reporting molecular dynamics simulations of HFC-134 and HFC-134a (CF_3CH_2F) in NaY. In these simulations, cations were found overall to migrate from the sodalite cages to the supercages according to a two-step mechanism: (1) a concerted two-cation jump from SI′ to SII′ (i.e., within the sodalite cage, the SII′ site being located at a 6-ring window opposite the SII site) and from SII to SIII/SIII′ and (2) a jump from SII′ to SII. As will be seen, our conclusions in this work are grossly consistent with these findings, although disagreeing in a number of details. Our simulations differ in two main aspects from those of Jaramillo et al. First, rather than $C_2H_2F_4$, the sorbate is chloroform, which will have an appreciably different mode of bonding to both framework and cations. Second, we follow a different simulation procedure. In our work, we apply a very standard atomistic MD method, but to a deliberately unrealistic situation: the first few picoseconds after the instantaneous sorption of a number of sorbate molecules. We carry out long, continuous simulation runs at three different temperatures, recording the fate of all sodium cations. We are thus able to follow migration events sequentially as they occur and to determine that different types of cation migration can occur on different time scales. We compare results from two different loadings, 40 and 10 molecules/unit cell. Finally, we remove all the guest molecules and demonstrate that the cation migration may, at least to a certain extent, be reversible.

We also point out that, throughout this work, only classical potentials are used to describe the interatomic interactions. This assumes that only physical adsorption takes place and that there is no chemical reaction between the chloroform molecule and the zeolite. In reality, however, a reaction has been found to occur in experiments by Sanchez-Sanchez et al.[18] on sodium-containing zeolites X and Y. The authors report the presence of CO and a decline in the presence of $CHCl_3$. However, when considering zeolite Y, it was found that this reaction occurs very slowly and only becomes detectable at temperatures of 419 K. Although we accept therefore that some reaction may take place in the real system, we are satisfied that the model is sufficiently realistic for the purposes of our study (i.e., the examination of cation motion during the sorption process).

Materials and Methods

Potential Parameters. The most important criteria in selecting a suitable force field for the simulations were (1) accurate description of the potential between the chloroform molecules and the zeolite framework, including sodium cations and (2) the ability to conduct molecular dynamics with a fully flexible framework. On the first count, we made use of the parameters reported by Mellot and Cheetham.[11] The short-range parameters were derived from those of argon (Cl terms) and methane (C and H terms), using appropriate scaling factors. The original Ar and methane potentials had accurately predicted the experimental heats of adsorption of those species in various zeolites. Moreover, the derived chloroform terms have been shown to reproduce accurately the heats of adsorption of chloroform in siliceous zeolite Y, NaY, and NaX across a range of loadings.[16] In these potentials, the short-range parts are given in the form of the Lennard−Jones 12-6 function

$$V(r) = 4\epsilon\left[\left(\frac{\sigma}{r}\right)^{12} - \left(\frac{\sigma}{r}\right)^{6}\right]$$

The short-range potential parameters, including those for the intermolecular interactions, are given in Table 1. In addition to the Lennard−Jones parameters, the potential also relies on

TABLE 1: Potential Parameters and Atomic Charges Used in the Molecular Dynamics Simulations

species	charge (e)	ref
Si	2.4	21
Al	1.4	21
O	−1.2	21
Na	1.0	
H	0.180	11
C	−0.102	11
Cl	−0.026	11

Buckingham Potentials

ion pair	A (eV)	ρ (Å)	C (eVÅ^6)
Si−O	30023.0	0.1621	12.840
Al−O	26998.0	0.1622	12.840
O−O	894.6	0.3244	0.0
Na−O	8200.0	0.218	11.8

Three-Body Potentials (Zeolite Framework)

atoms	k (eV rad^{-2})	θ_o (deg)	ref
O−Si−O	12.100	109.47	this paper
O−Al−O	2.200	109.47	this paper

Nonbonded Lennard−Jones Potentials

atom pair	ϵ (eV)	σ (Å)	ref
C−O	0.750232 E−02	3.25	11
H−O	0.780134 E−02	2.70	11
Cl−O	0.142532 E−01	3.43	11
C−C	0.222836 E−02	3.75	11
H−C	0.230329 E−02	3.36	11
C−Cl	0.479530 E−02	3.79	11
H−Cl	0.495729 E−02	3.39	11
Na−Cl	0.183103 E−01	2.90	11
Cl−Cl	0.103230 E−01	3.82	11
H−Na	0.983246 E−03	3.10	11
C−Na	0.114095 E−02	3.69	11

Harmonic Bonding Potentials

atom pair	k (eV)	r_o (Å)	ref
C−Cl	27.2511	1.761	34
C−H	29.5612	1.105	34

Three-Body Potentials (Intramolecular)

atoms	k (eV rad^{-2})	θ_o (deg)	ref
Cl−C−Cl	4.33652	109.50	34
H−C−Cl	5.81095	107.10	34

Coulombic terms. In the chloroform molecule, each of the atoms has a partial charge, based on Hartree−Fock calculations, with the charges scaled to reproduce the molecular dipole moment.[11] These charges are also given in Table 1. In the zeolite framework, the charge of oxygen must be −1.2 and that of Na is 1.0.

This leads to our second main concern, to obtain a robust description of the zeolite framework fully consistent with the zeolite−chloroform potentials. A number of framework force fields exist, covering a range of ionicities. The scheme where framework oxygen has a charge of −1.2 and Si +2.4 was first described by Kramer et al.,[21] where these charges were derived from SCF calculations. In their work, Al was assigned a charge of +1.4 and extraframework Na +1.0. The short-range interactions were described by Buckingham potentials. Auerbach and co-workers also derived a force field based on this charge scheme,[22] with a subsequently improved Na−O potential.[23] For our molecular dynamics simulations, we decided to derive a new zeolite framework force field based on the Kramer partial charge scheme, for the following reasons: (1) since we were interested in the migration of Na cations through zeolite pores, it was important to have as realistic a model of the framework as possible, including explicit Si−O and Al−O terms. The force field of Auerbach has an average T−O potential and works best with an average T atom charge. When used with the Kramer charges, we found that it underestimated framework bond lengths. (2) The potential should be robust to high-temperature simulations. The Buckingham potentials of both Auerbach and Kramer include very large C parameters (greater than 100 eV Å^6). At short interatomic separations, this can result in binding energies of unrealistically high magnitude, with consequential problems arising from the need to conserve total energy.

The new framework force field comprised Si−O, Al−O, O−O, and Na−O potentials, which were of the Buckingham form

$$V(r) = A \exp(-r/\rho) - Cr^{-6}$$

In addition, harmonic three-body terms were defined for the O−Si−O and O−Al−O intratetrahedral angles

$$V(\theta) = \frac{1}{2}k(\theta - \theta_0)^2$$

The Si−O potential was first derived by arbitrarily fixing the Buckingham C parameter to be 10 eV Å^6 and then fitting the other parameters such that the overall minimum of the function (including the Coulombic part) most closely approached that of the Kramer potential. An analogous procedure was adopted for the O−O terms, except that no C parameter was defined at all. These potentials were then further refined by being fit to the experimental crystal structures of quartz and siliceous MTW, MEL, and FER zeolites using the GULP program.[24] The resulting parameters are those given in Table 1. The Al−O potential was initially derived by scaling the A parameter of the Si−O potential and further improved by being fit to the experimental structures of zeolites MAP and NaY (see the next section for comparison of NaY cell parameters). At the same time, the Na−O potential and the framework three-body terms were refined. Again, all parameters are given in Table 1.

Finally, the chloroform intramolecular bonding and three body terms were represented by modified *cvff* parameters[34] and are listed in Table 1. The bonded terms are represented by a harmonic potential

$$V(r) = \frac{1}{2}k(r - r_0)^2$$

with the three-body potentials being simple harmonic functions, as for the framework.

Zeolite Model. The model of NaY used in the simulations had the composition $Na_{56}Si_{136}Al_{56}O_{384}$, based on the structure refined from powder X-ray diffraction data by Fitch et al.[35] The 56 sodium atoms per unit cell were distributed among the various possible sites as follows: 6 SI, 18 SI′, and 32 SII. The positions of the various cation sites are illustrated in Figure 1. Neighboring SI and SI′ sites were not allowed to be populated. Aluminum was also randomly distributed among the framework T sites, subject to Löwenstein's rule. The structure was energy minimized in the program GULP,[24] using the same potential parameters as were to be used in molecular dynamics, at constant pressure but with the constraint that the cell remained cubic. The lattice parameters of the unloaded NaY before and after the minimization are shown in Table 2. The zeolite was loaded with either 40 or 10 chloroform molecules using a Monte Carlo algorithm as implemented in the Cerius2 *Sorption* module[25] (40 molecules/unit cell being roughly equivalent to the equilibrium

TABLE 2: Simulated and Experimental Values of the NaY Lattice Parameters Volume after Energy Minimization

parameter	experimental value	simulated value	difference	units	percent
volume	15206.8074	15240.9284	34.1210	Å^3	0.22
A	24.7749	24.7935	0.0184	Å	0.07

loading at 1 atm and at 300 K). Prior to the molecular dynamics, the entire system underwent a further energy minimization using GULP, with the cell parameter fixed at the value for the minimized unloaded NaY.

Molecular Dynamics. The minimized cell dimensions were then kept fixed during the MD runs. MD was conducted using the program DL_POLY[26] in the NVT ensemble, using the Evans algorithm,[27] for at least 500 ps at each of three temperatures: 270, 330, and 390 K. During an initial 50 ps equilibration period, the Na cations were held fixed in their energy minimized positions. Analysis of subsequent MD runs showed that this did not adversely affect the conservation of energy during the simulation. All components of the system were then treated as fully flexible during the MD simulation.

Results and Discussion

Molecular dynamics simulations by Jaramillo and Auerbach[23] already indicated that the Na cations in unloaded NaY are essentially immobile at 300 and 1000 K. Simulations using our own model, not described here in detail, largely confirmed this result. Although a small number of cation displacements is observed at higher temperatures in the bare zeolite, there was no appreciable migration occurring. The results of the MD simulations presented here show that there is migration of the cations upon chloroform adsorption. Different types of motion are observed depending both on the location of the cation and on the time elapsed. It is important to note that many of the cation migrations appear to be irreversible within the time scale of the simulation in that they involve migration from sites inaccessible to the sorbate molecules into the larger cavities of the zeolite pore system. Therefore, although an equilibrium MD method has been used, results of the simulation evolve over the passage of time rather than representing a steady-state situation. The results presented are for the simulations run at 270, 330, and 390 K. There are four types of motion observed during the simulation.

Cation Motions. (i) Migration of SII Cations into the Supercage. Some cations located in the SII site migrate from their positions at the edge of the supercage toward the center. In the simulation cell, this part of the zeolite is crowded with chloroform molecules, and interaction of these polar molecules with the sodiums accounts for the migration of these particular cations, with the Na^+ being more favorably solvated by the chloroform molecules than by the zeolite framework. In certain instances, it is also observed that an SI′ cation begins to move into the supercage prior to any substantial migration of nearby SII cations. Therefore, electrostatic repulsion between sodium ions may also contribute to SII motion. For instance at 390 K, an SI′ cation moves to within 3.9 Å of an SII cation interacting with a sorbate molecule. This is similar to the simultaneous migration suggested by MD calculations on HFC-134 in NaY by Jaramillo et al.[20] However, not all migrations occurred in this way. The SII cations begin their migration early on in the simulation at all temperatures simulated; the mean square displacement (MSD) plots calculated for these particular cations reflect this (see Figure 2). The plots show that there are continuous migrations over a period of 70−90 ps together with

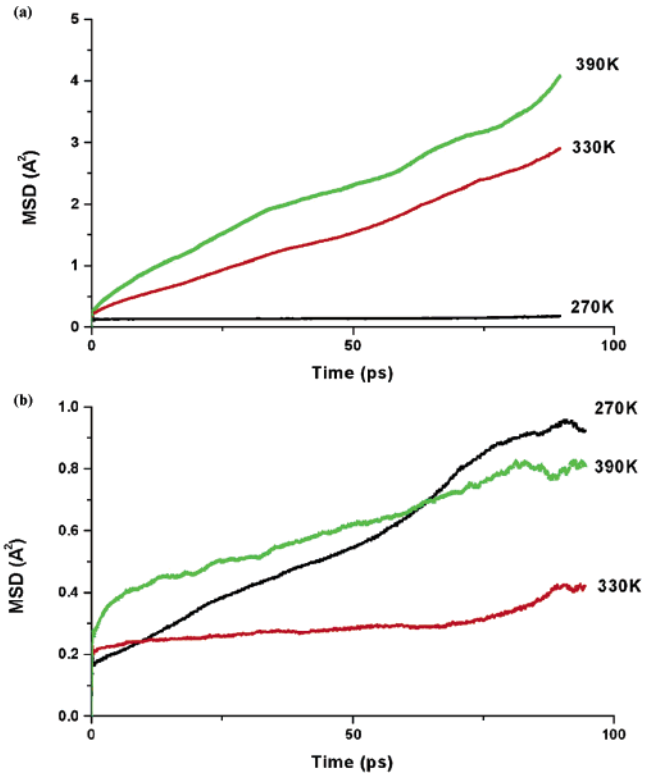

Figure 2. MSD plots for the SII Na cations (a) between 0 and 100 ps of MD simulation and (b) between 100 and 200 ps of MD simulation.

TABLE 3: Areas of Regions A and B from Figures 3 and 7

	0−100 ps	100−200 ps
	Region A	
SII−Cl	2.710	2.867
SI−Cl	0.451	0.575
	Region B	
SII−Cl	2.420	2.412
SI−Cl	0.749	0.849

shorter hops. The SII cations do not move back toward their initial positions and tend to become less mobile after a certain period of time, as seen in the decreasing scale of the MSD plots in successive time frames in Figure 2a,b. The original SII sodiums are held in new positions by a dual interaction between the oxygen atoms near two SIII′ sites and by the chloroform molecule. (It is important to note that throughout this work the description of SI, SI′, and SII cations refers only to their locations at the start of the simulation and not necessarily their position at any subsequent time.) The cation motion during the rest of the simulation may be described as thermal vibrations. Radial distribution function plots for the SII cations and chlorine atoms were calculated at 390 K between 0 and 100 ps of simulation and between 100 and 200 ps of simulation, and these are shown as Figure 3. Although the plots are very similar in terms of the positions of the first two peaks, integration of the plots to yield the summed $n(r)$ values (see Table 3) shows that there is a significant increase in area A (the area of first peak, which has a maximum at about 3.1 Å up to 4.5 Å) from the first to the second 100 ps, with the total coordination up to 4.5 Å changing significantly from 2.71 to 2.86. This demonstrates that, over time, more SII cations come into contact with chlorine atoms, consistent with the fact that the cations are moving away from their original SII sites. We also define an area B between 4.5 and 6.8 Å where a smaller peak corresponding to a second

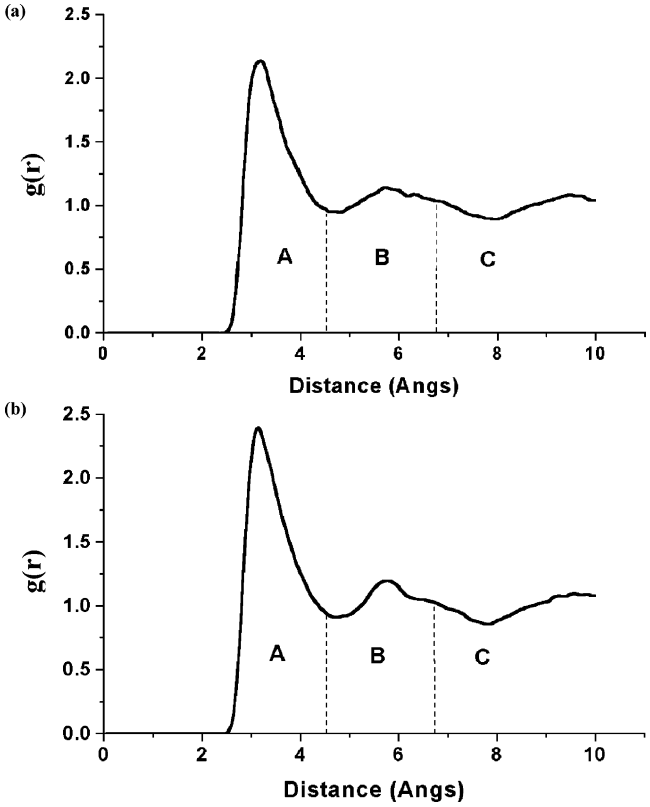

Figure 3. Radial distribution function plot for SII Na cations and Cl atoms, summed (a) between 0 and 100 ps and (b) between 100 and 200 ps of MD simulation at 390 K.

Na−Cl coordination shell is located. For the SII cations, the integrated area of this region changes very little from the first to the second 100 ps. Figure 4 illustrates the movement of SII cations over the initial 100 ps of production in the simulation.

(ii) Migration of SI′ Sited Cations into the SII Sites. Some cations in site I′ are observed to migrate from their position in the sodalite cage into the supercage and take up position at a vacant SII site, in the manner predicted by Grey et al.[12] using X-ray diffraction and NMR experiments, and as shown from the calculated MD trajectory in Figure 5. This involves the cation traversing a zeolite six-ring; a process predicted to have a high activation energy.[28] Recent work using molecular dynamics has indicated that such motion also occurs upon sorption of HFC-134 and HFC-134a. It was reported that the cation motion was SI′ to SII′ to SII.[20] Although the cations do pass through SII′ on the way out of the sodalite cage, the amount of time spent there is small, possibly due to a low energy barrier to jump from SII′ to SII. Our calculations,[29] using the defect energy minimization technique with the Mott Littleton scheme, have shown the presence of a potential energy well on both sides of the six-ring facing the supercage, corresponding to the SII and SII′ sites. The jump from SII′ to SII has a low energy barrier, hence the fairly rapid traversal seen in our MD simulations. The number of cations migrating is dependent on the temperature of the simulation, with seven SI′ cations per unit cell being seen to migrate into the supercage at 390 K over 500 ps.

At 270 K, two SI′ cations per unit cell migrate over the simulation time scale with the remainder staying within the sodalite cage. At 330 K, this number increases to three cations per unit cell. The process of a SI′ cation migrating to a SII site happens within a time period of about 5 ps and takes the form of a short hop across a six-ring into the supercage. The MSD plot for SI′ cations over this initial period, shown in Figure 6a, shows only the very short time scale hops consistent with this migration, except for the 390 K run, where the cations are seen to diffuse over a longer time scale within the first 100 ps of MD, this being consistent with the diffusional type of motion seen for the SII cations in the supercage. On the MSD plots, the hops are deemed to be the initial jump at 0 ps from 0 Å^2 to a low MSD value. Otherwise, the cations are essentially immobile for the first 100 ps at 330 and 270 K. This is in contrast to the motion of the SII cations in the first 100 ps at these temperatures. A possible explanation is that certain SII sites need to be vacated first to permit the SI′ cations to migrate into them. Also, the SII diffusion within the supercage will

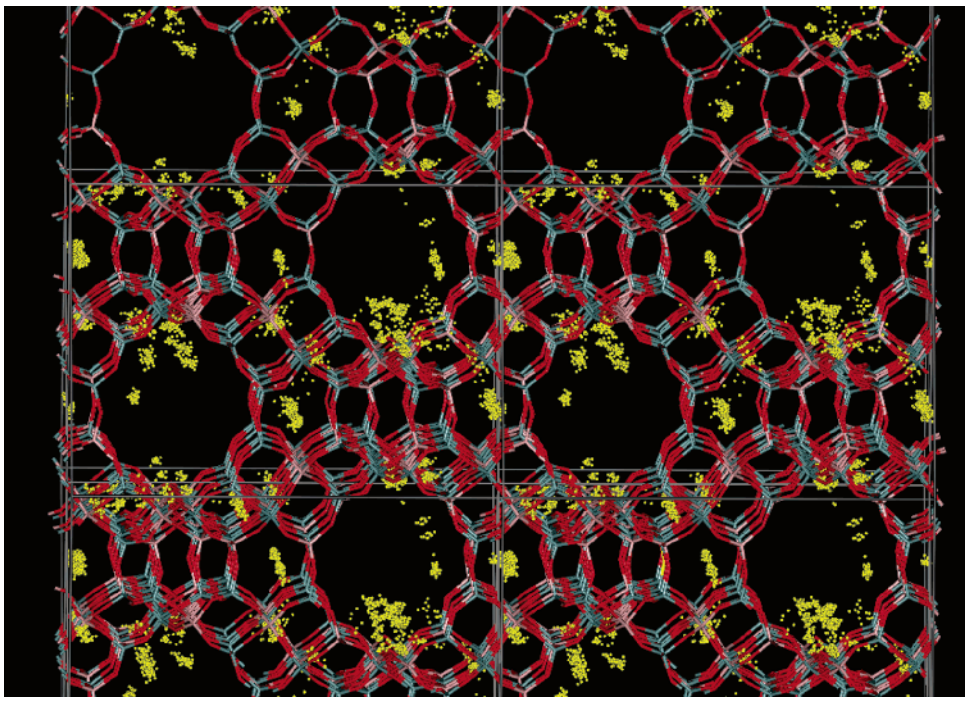

Figure 4. Superposition of SII Na cation locations (yellow) over the initial 100 ps of MD simulation (390 K), showing their migration toward the middle of the zeolite supercage. For clarity, the chloroform molecules are not shown in this diagram.

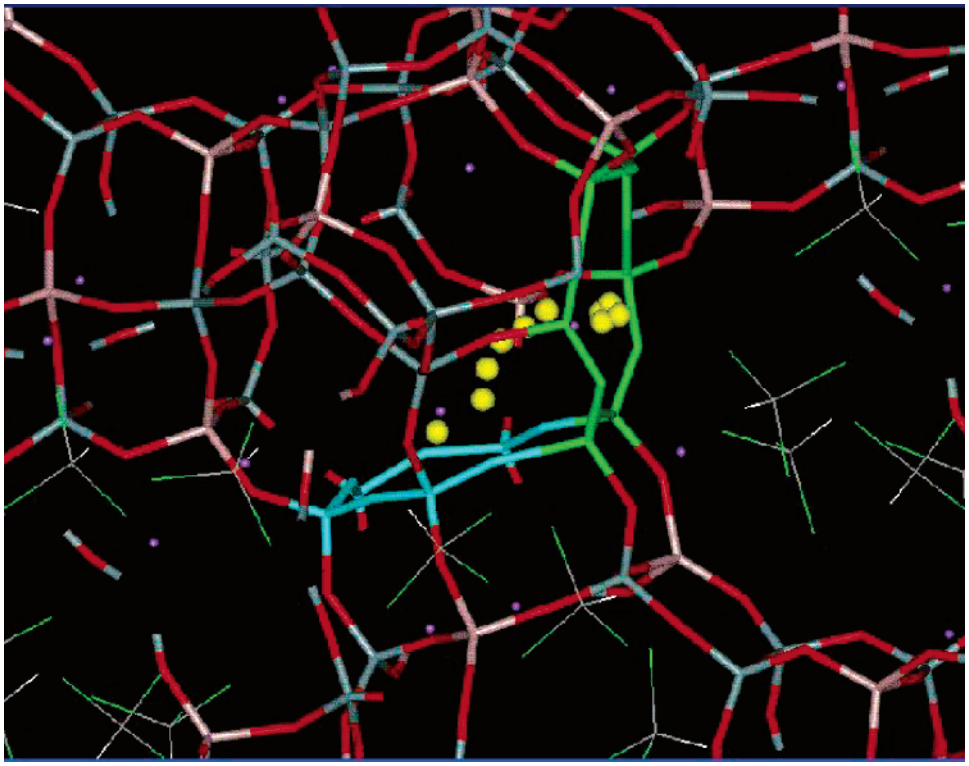

Figure 5. Migration path of sodium cation (yellow spheres) from an SI′ site to an SII site. The blue ring represents the six-ring associated with the SI′ site. The green ring highlights the six-ring facing the supercage, containing the SII site.

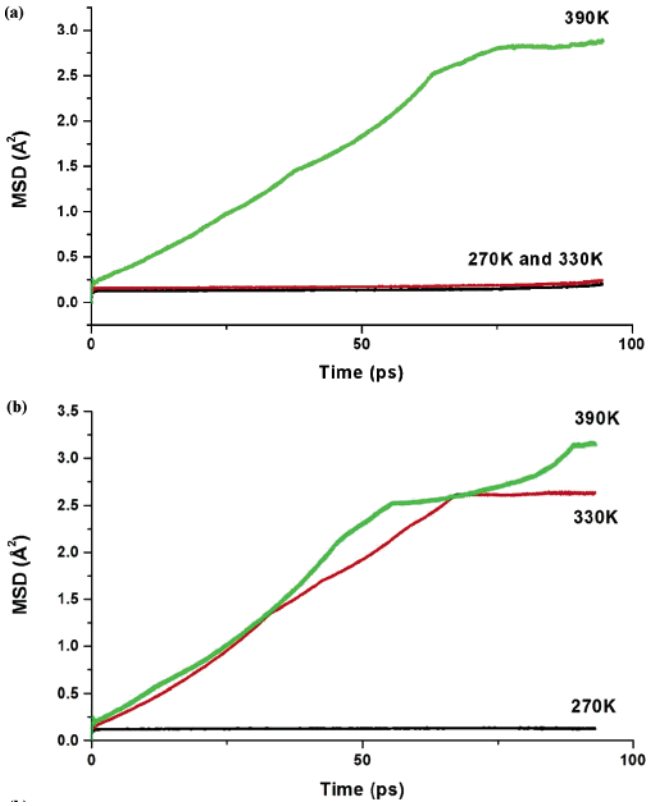

Figure 6. MSD plots for the SI′ Na cations (a) between 0 and 100 ps of MD simulation and (b) between 100 and 200 ps of MD simulation.

certainly have a lower energy barrier than migration of cations from within the sodalite cage, as no six-ring needs to be traversed, for example, in migration from SII to SIII′. After 100 ps, a combination of short hops and more continuous diffusion is observed, as shown by the MSD plot in Figure 6b. This represents both migration to the SII site and diffusion of the former SI′ cations now in the supercages. From the trajectory, it is evident that some cations migrate into vacant SII sites in the first 100 ps and also to recently vacated SII sites as also seen at the lower temperatures. Radial distribution functions between SI′ Na cations and Cl atoms calculated between 0 and 100 ps of the 390 K simulation, and between 100 and 200 ps (Figure 7), show an increase in total coordination between 0 and 4.5 Å (area A in Figure 7) from 0.45 to 0.57 comparing the earlier to the later time period, suggesting a continuing migration of SI′ cations into the supercage (see Table 3). The area of region B also increases from 0.75 to 0.85. For the SII cations, this was the area of the second maximum in the distribution function. Taken together, there is a significant increase in coordination of the SI′ cations by Cl, again consistent with the fact that some among them have migrated to locations where they may interact more closely with the chloroform molecules.

(iii) Migration of SI′ Cations to Vacant SI′ Sites. The third type of motion observed involved the concerted migration of SI′ cations. When one SI′ cation vacates its site and hops into the supercage, a second SI′ cation from a site within the same sodalite cage is sometimes observed migrating across the cage and taking up the original position of a cation that has migrated into the supercage. This has been observed to occur in the simulation at 330 K and takes place over a time scale of about 5 ps.

(iv) Migration of SI Cations to Vacant SI′ Sites. Analysis of the trajectories reveals that the SI cations are also more mobile after adsorption than in unloaded NaY. Some SI cations are observed migrating out of their original position in the double six-ring between the sodalite cages and into a nearby SI′ site. This is in accordance with the observation by Bosch et al.[17] that there is a decrease in site I population upon adsorption and that it occurs over a longer time period than the SI′ hopping motion (although the hopping process itself is rapid). SI cations

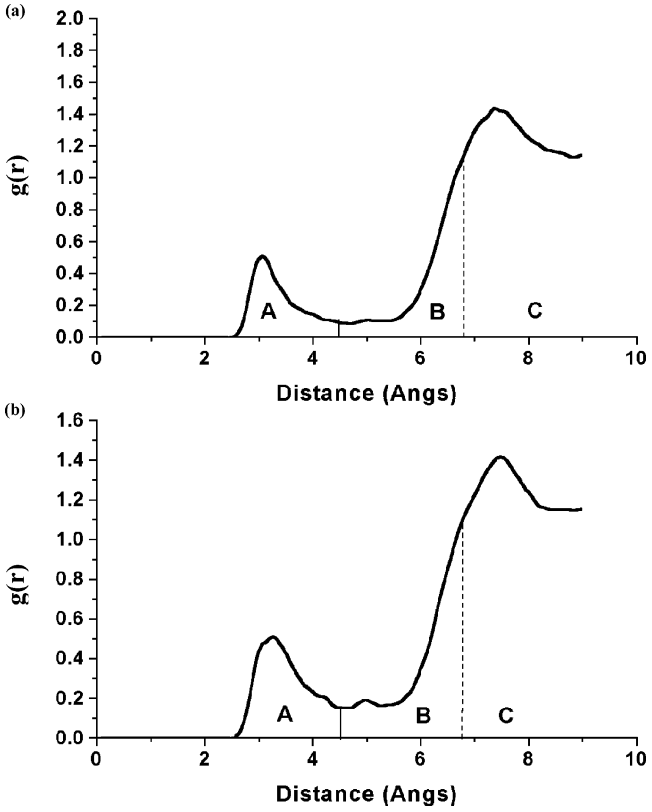

Figure 7. Radial distribution function plot for SI′ Na cations and Cl atoms, summed (a) between 0 and 100 ps and (b) between 100 and 200 ps of MD simulation at 390 K.

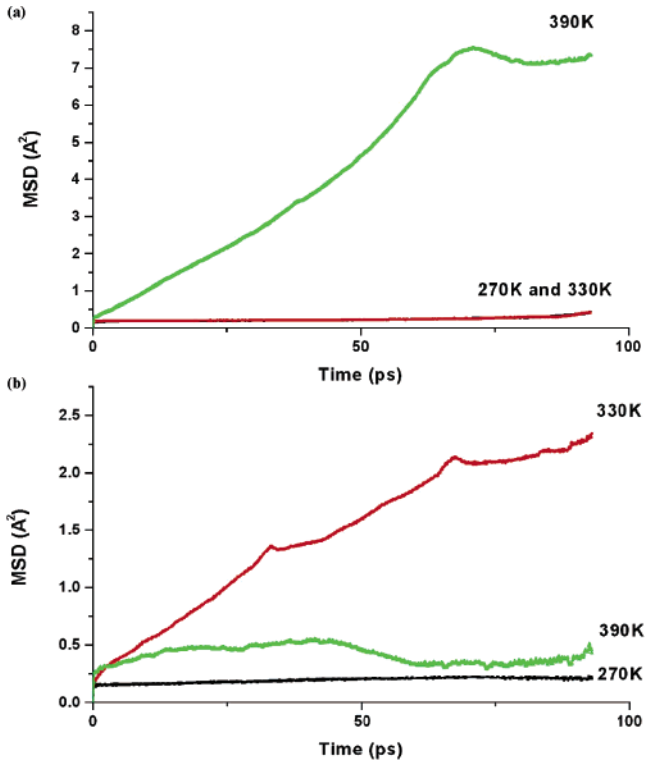

Figure 8. MSD plots for SI Na cations (a) between 0 and 100 ps of MD simulation and (b) between 100 and 200 ps of MD simulation.

are immobile during the first 100 ps of MD at 270 and 330 K in that there is no diffusive motion, as shown in Figure 8a. At 390 K, however, the cations are seen to migrate. Between 100 and 200 ps of simulation, the cations still do not exhibit diffusive

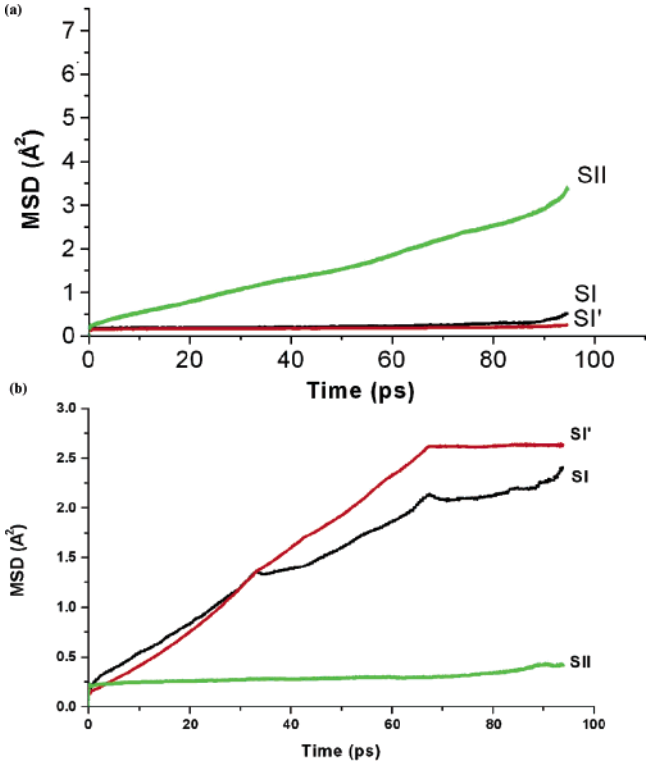

Figure 9. MSD plot for all Na cations (a) between 0 and 100 ps of MD simulation and (b) between 100 and 200 ps of MD simulation at 330 K.

motion at 270 K, although they are seen to be more mobile at 330,K during the same time period. This is reflected in the MSD plot in Figure 8b. We note here that the statistically small number of SI cations gives rise to the unevenness and cusps seen in the MSD plot (and also visible in Figure 9). Some cations hop into an SI′ site after 100 ps of simulation having initially been seen to remain in the double six-ring. Having entered the sodalite cage, the cations also subsequently hop within the sodalite cage in the manner described previously in (iii). During the simulation at 390 K, some SI cations that have hopped into SI′ sites then diffuse further into the supercage, via a vacant SII site, in the manner suggested for the SI′ cations. Although this is a rare event during the simulations, it may occur more frequently during a simulation of a longer time.

Diffusion of these cations toward the center of the supercage has not been observed in the simulations to the same extent as for the other cations, although longer simulation times may be necessary to observe this. The relative mobilities of the cations at 330 K are shown in Figure 9. The different types of motion described are summarized graphically in Figure 10.

Loading of 10 Molecules per Unit Cell. The simulations were also performed with 10 chloroform molecules per unit cell to study the effect on the cations of a lower sorbate loading. At all of the simulated temperatures, the cations were found to be comparatively immobile. Some cations were seen to migrate between sites, but this was restricted to only a few SII and adjacent SI′ sites and at a much smaller scale to that occurring with 40 molecules per unit cell. The fact that these were largely the same cations that migrated first during the simulation at higher loading could indicate that the local framework composition has a role in influencing the migration of these cations, in addition to that of the sorbate−cation interactions. In general, the results suggest that cation migration is dependent on the concentration of sorbate, with lower concentrations not being able to affect significant cation migration.

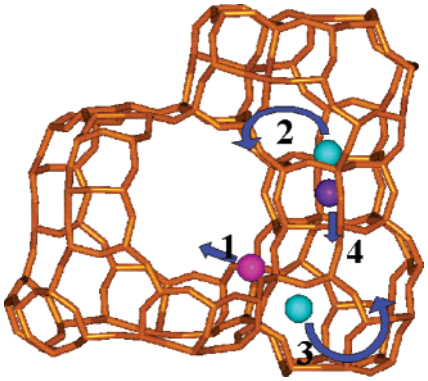

Figure 10. Graphic showing the various cation motions described. (1) Motion of SII cations toward the center of the supercage. (2) Hopping of SI′ cation into a site II position in the supercage. (3) Migration of SI′ cation across the sodalite cage into another SI′ site. (4) Hopping of the SI cation into a SI′ position.

Diffusion and Bonding of Chloroform Molecules. The diffusivity of the chloroform molecules is related to the loading and temperature. It is generally reported in other works using molecular dynamics that the rate of molecular diffusion increases with loading.[30] In our case, however, we have only examined two loadings, from which it appears that the diffusivity of the molecules is much lower at a loading of 40 molecules/unit cell, as compared to that at 10 molecules/unit cell. Since our main interest in this work was the migration of the extraframework cation, we have not examined a wider range of loadings. However, it is likely that 40 molecules/unit cell represents a level of saturation where the diffusion of sorbate molecules begins to become impeded by excessive collision between the molecules.

The calculated diffusion coefficients are given in Table 4, where the lower diffusivities at the higher loading may be seen. At both loadings, diffusivity increases with temperature, as expected. In general, these coefficients are lower than those calculated for other, less polar, hydrocarbons in zeolite Y and other zeolites. For instance, Yashonath et al.[31] performed molecular dynamics simulations on methane diffusing in both zeolites A and Y. The diffusion coefficients reported for the sodium zeolite Y case matched well with experimental data and were higher than those calculated here for chloroform for comparable loadings. Methane is a much less polar molecule that chloroform, and its interaction with the zeolite framework is weaker, being dominated by dispersive van der Waals' forces, even though the extraframework cations may polarize the molecules to some extent. In contrast, chloroform binds more strongly, both via electrostatic Cl−Na interaction and through hydrogen bonding between H and framework oxygen. Monte Carlo simulations made by us and others[16] indicate that these interactions may take place with oxygen atoms situated on a four-ring facing the zeolite supercage (approximately where an SIII or SIII′ site would be in zeolite X). Some of the molecules in our molecular dynamics simulations are orientated in such a way, and at such a distance, as to allow interaction with the cation and framework oxygen atoms, similar to Scheme 2 proposed by Bosch et al.,[17] and illustrated in Figure 11. This would help to account for the rapid and early motion of the SII cations with a loading of 40 molecules per unit cell and the fact that a smaller number of cations moves during molecular dynamics on a system containing only 10 sorbate chloroform molecules.

TABLE 4: Calculated Diffusion Coefficients for Chloroform in Zeolite NaY at Loadings of 10 and 40 Molecules/Unit Cell

	approximate diffusion coefficient (m2 s^{-1})	
T (K)	10 molecules/unit cell	40 molecules/unit cell
270	4.72×10^{-10}	2.55×10^{-12}
330	5.54×10^{-10}	2.92×10^{-12}
390	1.29×10^{-9}	5.98×10^{-11}

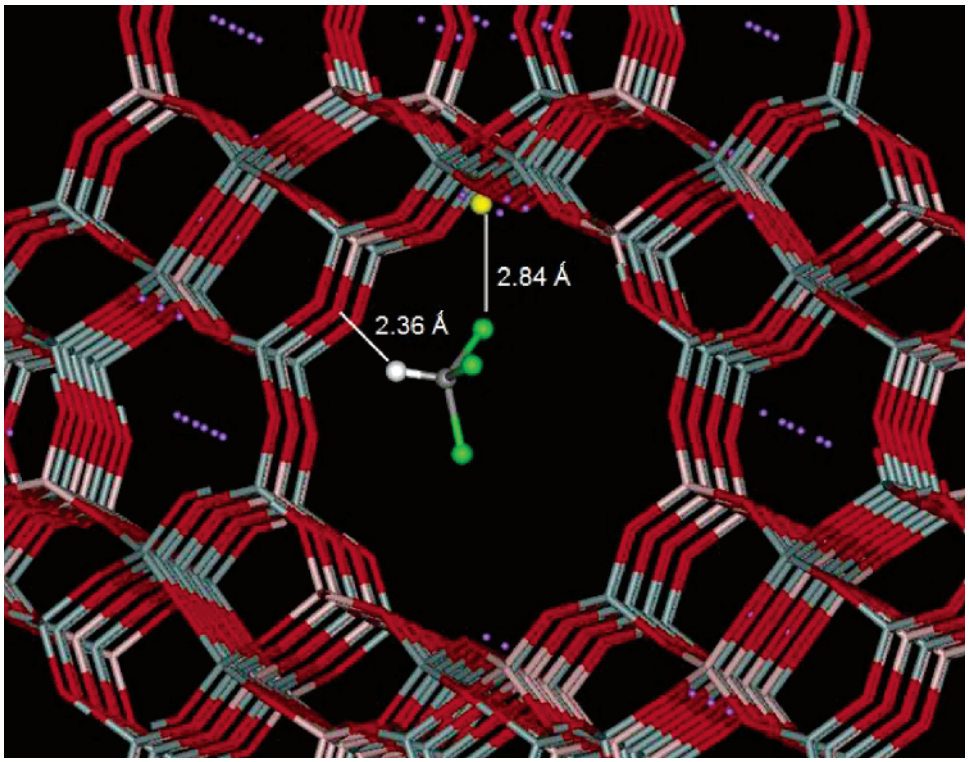

Figure 11. Sample configuration, taken from our simulations, showing the dual interaction of a chloroform molecule with the zeolite via both a weak hydrogen bond to framework oxygen and an electrostatic interaction between a chlorine atom (green spheres) and a sodium cation (the specific sodium is represented by a yellow sphere). The hydrogen atom on the $CHCl_3$ molecule is represented by a white sphere.

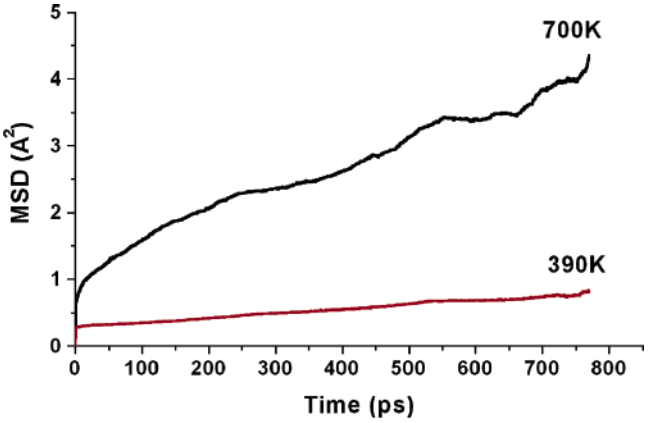

Figure 12. MSD plots for those Na cations that had originally migrated from SI′ sites into SII/supercage sites, after sorbate removal, at 700 and 390 K.

Evacuation of the Sorbates. Having performed simulations for at least 600 ps, the chloroform molecules were instantaneously deleted from the simulation cell, and the simulations were continued, at temperatures of 390 and 700 K, to study any possible redistribution of the cations. The simulations were run under the same conditions as for the sorbate-loaded cases and for at least 500 ps.

Analysis of the trajectories indicated that the migration of a cation from an SII site back to an SI′ site occurs in a number of cases. The mean square displacements for these cations reflect the observation that there is significant movement by some of the cations that originally occupied SI′ positions in the unloaded zeolite but entered the supercage upon chloroform sorption. In Figure 12, we show the MSD plots solely of these cations. Although it should be borne in mind that not all of these cations reenter the sodalite cages, the fact that it is only these cations that do so may indicate the relative stabilities of cations held in six-rings of differing aluminum contents. The SI cations are relatively immobile during this simulation.

For the simulation at 700 K, we also observed some cations that had been extracted from SII positions due to interactions with the sorbate molecules returning to their original sites. Many of these had found their way to positions where they were coordinated with either two oxygen atoms and/or were near SIII or SIII′ sites not normally found to be occupied in bare NaY zeolites. A reason for this is that the potential energy surface in this area is relatively flat. This is in accordance with the finding by Jaramillo and Auerbach[23] that cations located in SIII′ sites are mobile in NaX. Interestingly, this is only observed at six-rings where there is more than one aluminum atom present. The relative mobilities of the SII cations after sorbate evacuation at 390 and 700 K, as calculated from the MD runs, are shown in Figure 12.

Conclusions

Molecular dynamics simulations demonstrate that, at temperatures of 270, 330, and 390 K, the Na cations in NaY become mobile upon the adsorption of chloroform. The time scale on which the migrations occur depends on the initial site of the cation and the temperature of the simulation. The SII cations are observed migrating toward the center of the zeolite supercage, as they are drawn out by the presence of the chloroform molecules. The SI′ cations are seen to migrate in two ways: (1) SI′ cations hop from their sites into adjacent SII sites in the supercage and (2) SI′ cations move to fill those SI′ sites vacated by migration into the supercage. Some SI cations are seen to migrate into nearby SI′ sites and subsequently exhibit motion within the sodalite cages. At 390 K, some original SI cations are observed migrating further into the zeolite supercage and filling vacant SII sites.

Otherwise, SI cations remain in the double six-ring, evidence of which is shown in the trajectories calculated from the simulation. Over the time scale of the simulations, SI and SI′ cations that migrate into the supercage are not observed to diffuse toward the center of the supercage to the extent that the SII cations do. There is the possibility that this phenomenon may occur over longer simulation times or in the presence of more polar molecules.

Simulations in which the sorbate molecules were then evacuated from the cell indicated that, although the cations in a bare zeolite are generally thought to be immobile, this is not the case when they have been displaced from their preferred positions. Some cations were seen to return from SII-type sites to positions within the sodalite cages. Furthermore, cations at low-coordinate sites close to SIII or SIII′ in the supercage migrated back to SII sites, showing a strong preference for the six-ring site. The simulation results are consistent with the majority of experimental studies of halocarbons in NaY, discussed in the Introduction, and also with recent MAS NMR work by Sanchez-Sanchez and Blasco,[32,33] which suggested the migration of Li and Na cations upon adsorption of pyrrole in LiNaY and LiNaX zeolites. The mechanism proposed was also similar to that described in this paper, with the migration of SII cations away from their crystallographic sites due to interactions with the sorbate molecules and migration of SI′ cations into vacant SII sites.

Acknowledgment. N.A.R. thanks the EPSRC for a studentship, and R.G.B. thanks the Leverhulme Trust for funding. The authors also thank Teresa Blasco and Manuel Sanchez-Sanchez for useful discussions.

References and Notes

(1) Davis, R. J. *J. Catal.* **2003**, *216*, 396.
(2) Barthomeuf, D. *Catal. Rev.-Sci. Eng.* **1996**, *38*, 521.
(3) Savitz, S.; Siperstein, F. R.; Huber, R.; Tieri, S. M.; Gorte, R. J.; Myers, A. L.; Grey, C. P.; Corbin, D. R. *J. Phys. Chem. B* **1999**, *103*, 8283.
(4) Ciraolo, M. F.; Hanson, J. C.; Norby, P.; Grey, C. P. *J. Phys. Chem. B* **2001**, *105*, 2604.
(5) Crawford, M. K.; Dobbs, K. D.; Smalley, R. J.; Corbin, D. R.; Maliszewskyj, N.; Udovic, T. J.; Cavanagh, R. R.; Rush, J. J.; Grey, C. P. *J. Phys. Chem. B* **1999**, *103*, 431.
(6) Wieland, W. S.; Davis, R. J.; Garces, J. M. *J. Catal.* **1998**, *173*, 490.
(7) Ono, Y.; Baba, T. *Catal. Today* **1997**, *38*, 321.
(8) George, A. R.; Sanderson, J. S.; Catlow, C. R. A. *J. Comput.-Aided Mater. Des.* **1993**, *1*, 169.
(9) George, A. R.; Catlow, C. R. A.; Thomas, J. M. *J. Chem. Soc.-Faraday Trans.* **1995**, *91*, 3975.
(10) Davidson, A. M.; Mellot, C. F.; Eckert, J.; Cheetham, A. K. *J. Phys. Chem. B* **2000**, *104*, 432.
(11) Mellot, C. F.; Cheetham, A. K. *J. Phys. Chem. B* **1999**, *103*, 3864.
(12) Grey, C. P.; Poshni, F. I.; Gualtieri, A. F.; Norby, P.; Hanson, J. C.; Corbin, D. R. *J. Am. Chem. Soc.* **1997**, *119*, 1981.
(13) Mellot-Draznieks, C.; Rodriguez-Carvajal, J.; Cox, D. E.; Cheetham, A. K. *PCCP Phys. Chem. Chem. Phys.* **2003**, *5*, 1882.
(14) Kawai, T.; Yanagihara, T.; Tsutsumi, K. *Colloid Polym. Sci.* **1994**, *272*, 1620.
(15) Mellot, C. F.; Davidson, A. M.; Eckert, J.; Cheetham, A. K. *J. Phys. Chem. B* **1998**, *102*, 2530.
(16) Mellot, C. F.; Cheetham, A. K.; Harms, S.; Savitz, S.; Gorte, R. J.; Myers, A. L. *J. Am. Chem. Soc.* **1998**, *120*, 5788.
(17) Bosch, E.; Huber, S.; Weitkamp, J.; Knozinger, H. *PCCP Phys. Chem. Chem. Phys.* **1999**, *1*, 579.
(18) Sanchez-Sanchez, M.; Blasco, T.; Rey, F. *PCCP Phys. Chem. Chem. Phys.* **1999**, *1*, 4529.
(19) Ramsahye, N. A.; Bell, R. G. *Stud. Surf. Sci. Catal.* **2001**, *135*, 16P14.

(20) Jaramillo, E.; Grey, C. P.; Auerbach, S. M. *J. Phys. Chem. B* **2001**, *105*, 12319.
(21) Kramer, G. J.; Farragher, N. P.; Van Beest, B. W. H.; Van Santen, R. A. *Phys. Rev. B* **1991**, *43*, 5068.
(22) Auerbach, S. M.; Henson, N. J.; Cheetham, A. K.; Metiu, H. I. *J. Phys. Chem.* **1995**, *99*, 10600.
(23) Jaramillo, E.; Auerbach, S. M. *J. Phys. Chem. B* **1999**, *103*, 9589.
(24) Gale, J. D. *J. Chem. Soc.-Faraday Trans.* **1997**, *93*, 629.
(25) *Cerius2 v. 4.2*; Accelrys, Inc.: San Diego, 1999.
(26) Smith, W.; Forester, T. R. *J. Mol. Graph.* **1996**, *14*, 136.
(27) Evans, D. J.; Morriss, G. P. *Comput. Phys. Rep.* **1984**, *1*, 297.
(28) Catlow, C. R. A.; Bell, R. G. *Solid State Ionics* **1994**, *70*, 511.
(29) Ramsahye, N. A. Computer modeling of halocarbon sorption in zeolite Y, Ph.D. Thesis, University of London, 2003.
(30) Demontis, P.; Suffritti, G. B. *Chem. Rev.* **1997**, *97*, 2845.
(31) Yashonath, S.; Demontis, P.; Klein, M. L. *J. Phys. Chem.* **1991**, *95*, 5881.
(32) Sanchez-Sanchez, M.; Blasco, T. *Chem. Commun.* **2000**, 491.
(33) Sanchez-Sanchez, M.; Blasco, T. *J. Am. Chem. Soc.* **2002**, *124*, 3443.
(34) Hagler, A. T.; Lifson, S.; Dauber, J. *J. Am. Chem. Soc.* **1979**, *101*, 5122.
(35) Fitch, A. N.; Jobic, H.; Renouprez, A. *J. Phys. Chem.* **1986**, *90*, 1311.